Arabian Journal of Chemistry (2020) 13, 6236–6245

King Saud University

Arabian Journal of Chemistry

www.ksu.edu.sa
www.sciencedirect.com

ORIGINAL ARTICLE

Synthesis, antibacterial evaluation, *in silico* ADMET and molecular docking studies of new N-acylhydrazone derivatives from acridone

Mohammed Aarjane [a,*], **Adnane Aouidate** [b], **Siham Slassi** [a], **Amina Amine** [a]

[a] *Laboratory of Chemistry/Biology Applied to the Environment, Faculty of Science, University Moulay Ismail, BP 11201 Zitoune, Meknes, Morocco*
[b] *Laboratory of Molecular Chemistry and Natural Substances, School of Sciences, Moulay Ismail University, Morocco*

Received 3 April 2020; accepted 27 May 2020
Available online 3 June 2020

KEYWORDS

Acylhydrazone;
Acridone;
Antibacterial;
Docking;
ADMET

Abstract Novel N-acylhydrazone derivatives from acridone have been synthesized by condensation of acridone acetohydrazide and various aldehyde. The novel acylhydrazones were tested for their *in-vitro* antibacterial activity against human pathogenic strains. The MIC results indicate that compound **3f** displayed high antibacterial potential against *Pseudomonas putida* with MIC = 38.46 μg/mL, which is very close to that obtained with the commercial antibiotic. The synthesized compounds were subjected for docking studies to understand the interaction of our compounds and transcriptional regulator enzyme of *pseudomonas putida* and DNA gyrase complex of *Staphyloccocus aureus*.

1. Introduction

Acylhydrazone compounds are important chemical intermediates used in the preparation of many heterocyclic skeletons and they are also interesting ligands for the formation of metal complexes (Areas et al., 2017), some acylhydrazone derivatives are used as highly sensitive and selective sensor of several metals (Aarjane et al., 2020; Liao et al., 2017). Acylhydrazone derivatives are reported for their pharmacological activities such as antibacterial (He et al., 2017; Wang et al., 2012), anticonvulsant (Dehestani et al., 2018), anti-inflammatory (Cerqueira et al., 2019; Kheradmand et al., 2013), antimalarial (dos Santos Filho et al., 2016; Inam et al., 2014; Tsafack et al., 1996) and antileishmanial activities (Coimbra et al., 2019). The versatility of acylhydrazones is related to the presence of geometrical isomers Z and E of the plane of the C═N bond of the fragment conformers acylhydrazone, as well as cis/trans at the amide function (Hamzi et al., 2016; Himmelreich et al., 1993; Podyachev et al., 2007; Sarigöl et al., 2015). Moreover, acridone nucleus constitute an important class of natural products that serve as chemical intermediates used in the preparation of many alkaloids such as Acronycine, Cystodytin A and Pyridoacridine (Gensicka-Kowalewska et al., 2017). Acridone and acridine are known for many years for their pharmacolog-

* Corresponding author.
E-mail address: m.aarjane@edu.umi.ac.ma (M. Aarjane).
Peer review under responsibility of King Saud University.

ELSEVIER Production and hosting by Elsevier

https://doi.org/10.1016/j.arabjc.2020.05.034
1878-5352

ical activities such as antimicrobial (Aarjane et al., 2019; Kudryavtseva et al., 2015), antimalarial (Kumar et al., 2009), antiviral (Sepúlveda et al., 2012) and antitumor bioactivity (Tillequin and Koch, 2005).

Nowadays, the resistance of pathogenic bacteria to the therapeutic antibiotics is considered as major public health problem (Abubakar et al., 2020; "Antibiotic Development: the Battle to Overcome Antibiotic Resistance," 1984; Zarei-Baygi et al., 2020), the multidrug-resistance in bacteria is increasing at a worrying percentage and it causes mortality in hospitals. As a result, there is a need to develop new compounds with diverse mechanisms of action to fight the increasing danger of drug-resistant bacteria. One of the promising approaches, in our opinion is to develop new antibacterial compounds by the introduction of acylhydrazone groups into the acridone skeleton. In the present work, we report the synthesis of novel N-acylhydrazone derivatives from acridone, antibacterial investigations of the synthesized compounds were performed towards four pathogenic bacteria. Moreover, docking studies of our compounds revealed that, occupation of our compounds the binding pockets of subunit GyrB (DNA gyrase, PDB ID: 3TTZ) of *Staphyloccocus aureus* and transcriptional regulator enzyme of *pseudomonas putida* (PDB ID: 2XUI) via hydrophobic and hydrogen bonding interactions may be the reason for its significant *in vitro* antibacterial activity.

2. Result and discussion

2.1. Synthesis

The synthesis of novel acylhydrazones based on acridone compounds was depicted in Scheme 1. Initially acridone was reacted with ethyl 2-bromoacetate using potassium carbonate and Tetra butylammonium bromide (TBAB) as phase transfer catalyst in DMF at 70 °C. The treatment of the ethyl ester (**1**) with hydrazine afforded the compound (**2**). The condensation reaction of the compound (**2**) with variously substituted aldehydes and ketone in ethanol give the expected new acylhydrazones **3a-k** in good yields.

The structure of these compounds was ascertained by ^{1}H NMR, ^{13}C NMR, IR and mass spectral data. The IR spectra of compounds **(3a-k)** showed characteristic absorption bands in the region of 1600–1611 cm^{-1} corresponding to the vibration of the imine function (C═N), and two bands corresponding to the stretching vibrations of the carbonyls of the acridone ring and the hydrazone function in the region of 1638 and 1680 cm^{-1}, respectively. However the desperation of the vibration bonds of amine (NH_2) group in the region of 3226 cm^{-1} confirmed the formation of compounds.

^{1}H NMR spectra of the compounds **(3a-h)** in DMSO d_6, gave two sets of resonance signals which can be attributed to the existence of conformational isomers in DMSO d_6 (*E*,*trans* and *E*,*cis*) (Fig. 1). The splitting of signals were observed for amide (CON**H**) between 12.10 and 11.77 ppm, methylene (NC**H**2) to 5.80–5.17 ppm and imine between 8.50 and 8.07 ppm (N═C**H**). In the compound **3k**, the isomerization around the double bond (C═N) is degenerated. Thus, the duplication of signals to 5.59–5.36 ppm and 10.77–10.66 ppm in the ^{1}H NMR spectrum can be attributed to the existence of cis/*trans*-amide conformers only. In ^{13}C NMR, the spectra also show two sets of signals to 47.11–48.50 ppm and 168.94–163.38 ppm corresponding to the signal of the methylene (—N—**C**H_2—) and amide (—NH**C**O), respectively, while the signal of the imine (**C**═N) to 149.85–145.30 ppm appears as a single signal.

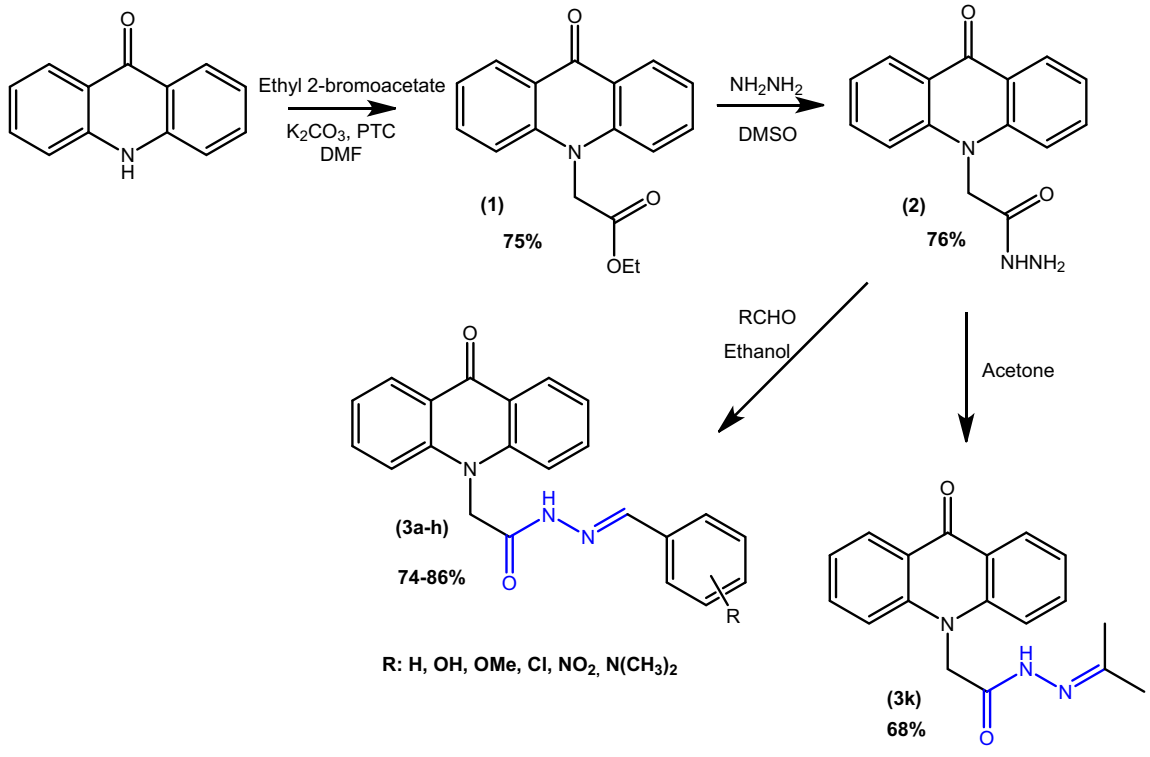

Scheme 1 Synthesis route of novel N-acylhydrazone derivatives from acridone (3a-k).

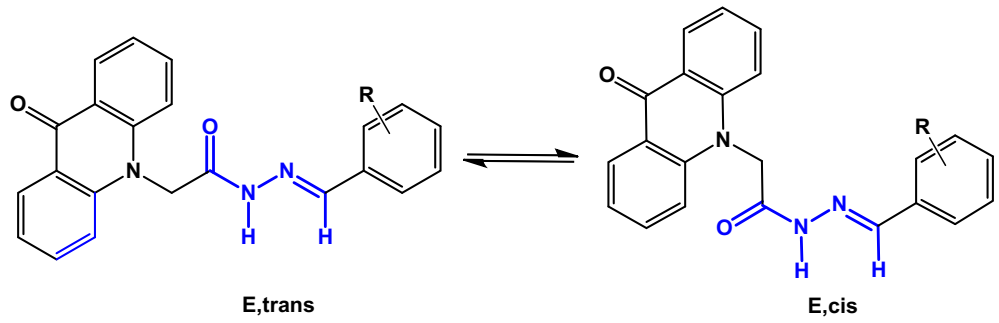

Fig. 1 *E,trans* and *E,cis* conformations in acylhydrazone derivatives.

The ^{1}H NMR spectrum of the compound **3a** shows two signals at 5.80 and 5.35 ppm attributable to the protons of the methylene (NC**H$_2$**), the signal at 5.80 ppm corresponds to the *E, trans* conformation with 73% abundance and the signal at 5.35 ppm assigned to the *E*, *cis* conformation with an abundance of 27%. Approximately the same abundance is found in the case of amide proton (CON**H)** at δ 12.01 ppm (23%, *E*, cis conformation) and 11.97 ppm (77%, *E*, *trans* conformation) and for the imine proton (N=C**H)** signals at δ 8.33 ppm (25%, *E*, *cis* conformation) and δ 8.18 ppm (75%, *E*, *trans* conformation). The signal intensities of the methylene, imine and amide protons allowed us to measure the ratio of cis/*trans*-amide conformers of **3a-h**, the percentage of cis/trans conformers in DMSO d_6 are summarized in Table 1.

2.2. Antibacterial activity

The novel acylhydrazone **(3a-k)** were tested for their *in vitro* antibacterial activities against the human pathogens three gram negative bacteria *Pseudomonas putida, Klebsiella pneumonia* and *Escherichia coli* and one gram positive bacteria *Staphyloccocus aureus*. The purity of compounds **(3a-k)** was confirmed by HPLC.

As revealed from Table 2, the compounds **3a**, **3b** and **3e** were found to have good antibacterial activity against *Staphylococcus aureus*, the compound **3a** was found to be the best active derivatives with MIC = 19.61 μg/mL. Moreover, the compound **3f** showed high antibacterial potential against *Pseudomonas putida* (38.46 μg/mL) which is very close to that obtained with the commercial antibiotic Chloramphenicol (37.03 μg/mL). The tested compounds **3a-k** shown moderate activity against *Escherichia coli* with the MIC values between 38.46 and 74.0 μg/mL. The low antibacterial activity was observed against *Klebsiella pneumonia*. The results indicate that the substitution of the acridone ring with acylhydrazone increase the antibacterial activity against all bacteria. Moreover the N-acylhydrazone acridone derivatives **3a-h** containing a secondary aldimine fragment showed interesting antibacterial activity compared with the **3k** derivative containing a secondary ketimine.

Table 1 E, *cis*/*trans* conformer ratios in DMSO d_6.

Compound	*E, cis (%)*	*E, trans (%)*
3a	27	73
3b	41	59
3c	26	74
3d	24	76
3e	26	74
3f	27	73
3g	28	72
3h	27	73
3k	33	67

2.3. In silico studies

To better, understand as well as to support the *in vitro* antibacterial activity of the synthesized compounds for the rational design of new potent molecules. In this manuscript molecular docking studies of the most active compounds have been made to study the interactions and clarify the probable binding modes between acridone derivatives and DNA gyrase complex (PDB ID : 3TTZ) of *Staphyloccocus aureus*, and transcriptional regulator (TtgR) enzyme (PDB ID : 2UXI) of *pseudomonas putida,* which provide straightforward knowledge for further structural optimization.

2.4. Docking for DNA-gyrase of Staphyloccocus aureus

The docking studies were carried out using the bacterial DNA gyrase complex obtained from Protein Data Base (PDB ID 3TTZ) (Sherer et al., 2011). Validation of the docking process was done by redocking of the co-crystalized ligand (07 N) to the ATP binding site of DNA gyrase and RMS (Root Mean Square) distance between the docked and the experimental co-crystallized binding pose was only 1.63 Å (less than 2 Å), which is satisfactory. Fig. S31 shows that the docked structure (magenta color) and the X-ray crystal structure (green color) are quite similar. In addition, all the eight acridones were docked into the binding pocket of DNA gyrase enzyme successfully. The molecular docking representation for each synthetic compound and the superposition of all best docking pose in the enzyme binding pocket are shown in Figs. S32-S33 (supplementary data).

Surflex-dock module from Sybyl-X 2.0 software (Tripos International, 2012) was used to predict the proposed binding mode, binding affinity, preferred orientation of each docking pose of the synthesized compounds with DNA gyrase structure. The calculated interaction energies for the synthesized compounds were in agreement with experimental result which showed that **3a**, **3b**, **3c**, **3d**, **3e**, **3f**, **3g** and **3h** are potent inhibitors of DNA-gyrase as compared to the other members and reference standard.

Table 2 Antibacterial data for the synthesized compounds (**3a-k**).

	S. aureus	*E. coli*	*K. pneumoniae*	*P. putida*
Acridone	122.83	133.41	137.93	156.31
3a	19.61	47.62	82.57	56.60
3b	29.13	38.46	130.43	99.10
3c	38.46	74.07	115.04	90.91
3d	38.46	56.60	115.04	65.42
3e	29.13	65.42	90.91	82.57
3f	47.62	56.60	90.91	38.46
3g	38.46	47.62	74.07	56.60
3h	47.62	65.42	82.57	74.07
3k	67.62	88.46	74.07	122.81
Chloramphenicol	11.65	22.41	15.38	37.03
Amx/A.Clavc	7.84	19.04	22.64	32.71
DMSO	–	–	–	–

Amx/A.Clavc : Amoxicilline/Ac Clavulanique (8/1).

It has been revealed from binding studies that all the synthesized compounds **3a-3h** fit snugly making various close contacts with the residues lining the active site of DNA gyrase.

It presented important interactions with the DNA-gyrase complex. The acridone moiety was involved in aromatic stacking interactions with Pro87 and Pi-cation with Arg84. The NH group of the amide group formed a hydrogen bond with the Thr173. Also, the benzene aromatic ring was involved in Pi-Alkyl interaction with Ile86. Hence, docking studies revealed the strong binding affinity of **3a** at the ATP binding site of GyrB, which may be responsible for its significant *in vitro* antibacterial activity especially against *S. aureus*.

Compound **3e** showed a binding affinity (-log ki) value of 6.16. The acridone moiety was involved in Pi-Anion and Pi-Cation interactions with Glu58 and Arg84. The NH of the amide group formed a hydrogen bond with Asn54. Moreover, the carbonyl of the acridone moiety formed a hydrogen bond with Gly85.

The proposed binding mode of compound **3b** showed a binding affinity value of 6.15. The acridone moiety was involved in hydrophobic interactions with Ile85, Ile102 and Ile175. Its carbonyl of the amide group formed a hydrogen bond with Thr173. In addition, the benzene ring showed a Pi-Alkyl interaction with Pro87.

From the different interactions of the synthesized compounds in Fig. 2, Table 3 and Figs. S32-S39, it can be concluded from the docking results that the eight compounds had H-bond interactions with the receptor indicating that the H-bond interactions play an important role of the inhibition of the DNA-gyrase. Additionally, they all bind to ATP binding site of DNA gyrase and share largely homogeneous in binding mode (especially hydrogen bond with Asn54, Arg144 and Thr173) to several DNA-gyrase inhibitors reported in the literature (Alves et al., 2014; Baig et al., 2015), Therefore, that can prove our docking process was reasonable. While the main cause of their mediated antibacterial activity is considered due to those compounds are aligned adequately within the ATP binding site of DNA-gyrase, which allows them to make important interactions with this pocket. The results of antibacterial activity are supported by docking analysis. The high docking scores and binding pattern of compounds of **3a**, **3b**, **3c**, **3d**, **3e**, **3f**, **3g** and **3h**, in Fig. 2, Table 3 and Figs. S32-S39, reveal that these compounds are well accommodated in active site of enzyme and they strongly interact within the active site of DNA gyrase enzyme (3TTZ). The molecules **3b**, **3c**, **3d**, **3f**, **3g** and **3h** were found to be orienting in opposite direction of compounds **3a** and **3e** as shown in supporting information Figs. S32-39.

2.5. Docking for transcriptional regulator (TtgR) enzyme of pseudomonas putida

For *pseudomonas putida* antibacterial activity the docking studies were carried out using the bacterial the transcriptional regulator (TtgR) enzyme (PDB Code: 2UXI) (Alguel et al., 2007) obtained from Protein Data Base.

In order to validate the docking approach, the co-crystallized ligand (Phloretin) was docked to the active site of the studied enzyme and RMS (Root Mean Square) distance was calculated, which was found 0.70 Å. (less than 2 Å), which is satisfactory. Fig. S40 shows that the docked structure (magenta color) and the X-ray crystal structure (green color) are quite similar. In addition, all the eight acridones were docked into the binding pocket of DNA gyrase enzyme successfully. The molecular docking representation for each synthetic compound and the superposition of all best docking pose in the enzyme binding pocket are shown in Figs. S41-S48 (supplementary data).

The Surflex-dock module was used to predict the proposed binding mode, affinity, preferred orientation of each docking pose and binding affinity of the synthesized compounds with transcriptional regulator (TtgR) enzyme. The calculated interaction energies for the synthesized compounds were in agreement with experimental result which showed that **3a**, **3b**, **3c**, **3d**, **3e**, **3f**, **3g** and **3h** are potent inhibitors of transcriptional regulator (TtgR) enzyme as compared to the other members and reference standard.

From the analysis of the active site of TtgR, it was observed that the residues Cys 137 and Asn110 along with Ala 74, Ser 77, Glu 78, Val 96, Ile 175 and VAL171 seem to play crucial role in binding with the ligands and triggering the efflux pump. The residues Asn 10 and Cys 137 probably are the most instrumental in binding through strong H-bonding and sensing the compounds toxic to the organism (Table 4 and Fig. 3).

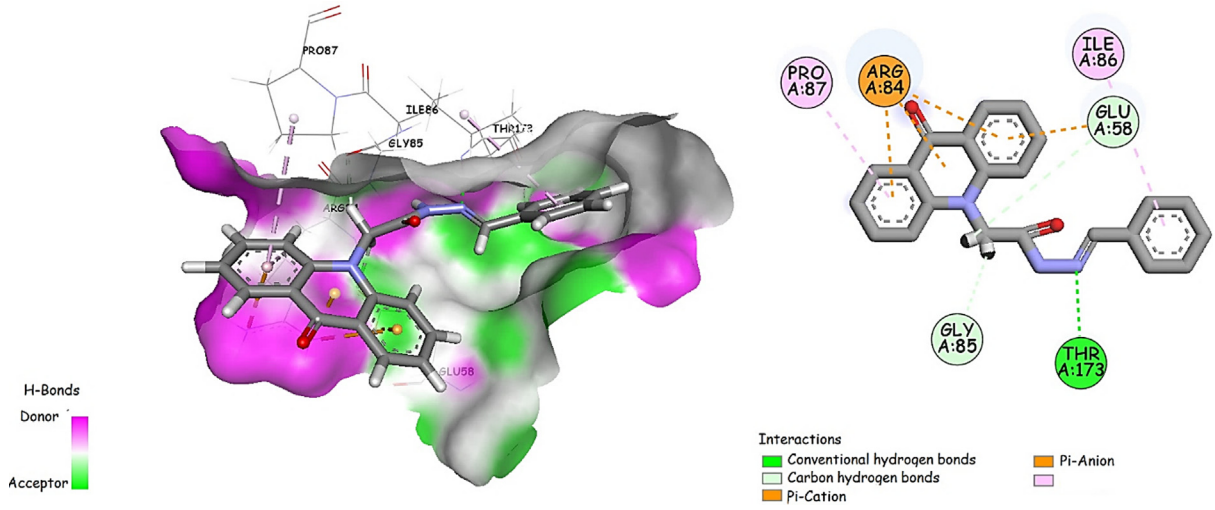

Fig. 2 Binding mode of compound **3a** with DNA-gyrase complex, the hydrogen bonds are presented in green dashed lines.

Table 3 The interactions and binding affinities between the eight synthesized compounds and DNA-gyrase of *Staphyloccocus aureu*.

	3a	3e	3c	3b	3h	3d	3g	3f
Hydrogen bonds	Thr173	Asn54 and Gly85	–	Thr173	Thr173	–	Arg144	–
Binding affinity (-log ki)	6.33	6.16	5.53	6.15	4.92	5.78	5.76	4.82

Table 4 The interactions and binding affinities between the eight synthesized compounds and transcriptional regulator (TtgR) enzyme of *Staphyloccocus aureu*.

	3a	3e	3c	3b	3h	3d	3g	3f
Hydrogen bonds	Asn 110 and Cys 137	–	–	–	Val 96 and Cys 137	–	Cys 137	Asn 110 and Cys 137
Binding affinity (-log ki)	6.26	4.67	4.62	4.55	5.95	5.01	6.38	6.622

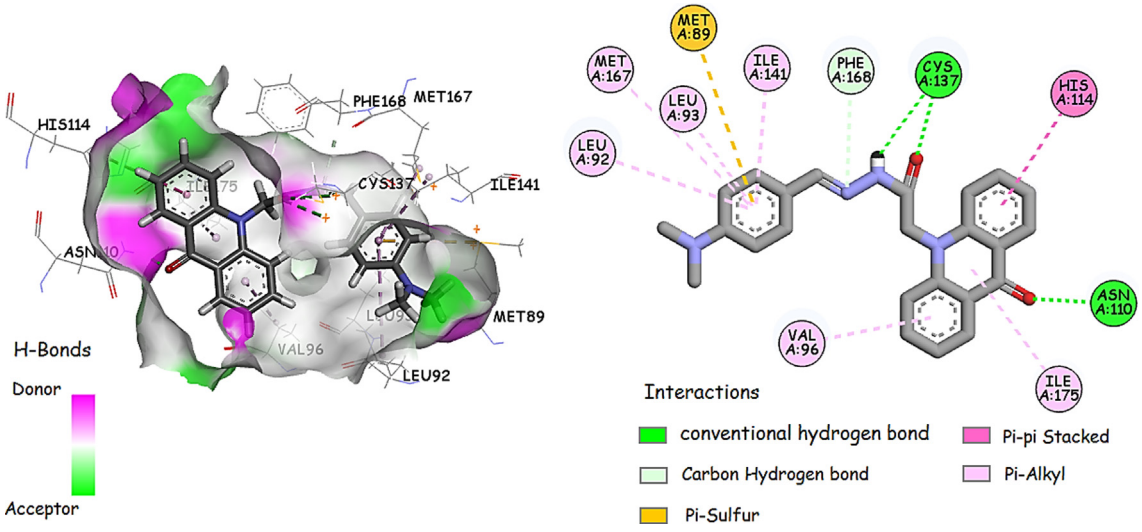

Fig. 3 Binding mode of compound most active compound **3f** with TtgR enzyme.

Table 5 In silico ADMET prediction of newly synthesized compounds.

Name	Absorption		Distribution	Metabolism							Excretion	Toxicity			
	Water solubility	Intestinal absorption (human)	Blood brain barrier Permeability	CYP							Total Clearance	hERG inhibitor	Max. tolerated dose (human)	Minnow toxicity	Skin Sensitization	AMES
				2D6 substrate	3A4 substrate	1A2 inhibitor	2C19 inhibitor	2C9 inhibitor	2D6 inhibitor	3A4 inhibitor						
	(log mol/L)	Numeric (% Absorbed)	(logBB)	Categorical (Yes/No)							Numeric (log ml/min/kg)	(Yes/No)	log(mg/kg/Day)	log(LC50)	(Yes/No)	(Yes/No)
the assayed compounds																
3a	−4.91	97.24	0.030.03	No	No	Yes	Yes	No	No	No	0.72	No	0.05	1.12	No	Yes
3d	−4.96	95.58	0.03	No	No	Yes	Yes	Yes	No	Yes	−0.05	No	0.04	1.44	No	Yes
3f	−5.32	98.10	−0.22	No	Yes	Yes	Yes	No	No	Yes	0.83	No	0.37	0.33	No	Yes
3g	−4.85	95.34	−0.61	No	No	Yes	Yes	No	No	No	0.67	No	0.02	0.91	No	Yes
3e	−4.98	97.69	−0.20	No	No	Yes	Yes	Yes	Yes	Yes	0.72	No	0.49	0.18	No	Yes
3b	−4.00	94.43	−0.23	No	Yes	Yes	Yes	No	No	No	0.62	No	0.15	0.68	No	Yes
3c	−4.81	94.65	−0.23	No	No	Yes	Yes	Yes	No	Yes	0.62	No	0.38	0.70	No	Yes
3h	−4.13	92.59	−0.24	No	Yes	Yes	Yes	Yes	Yes	No	0.56	No	0.03	1.06	No	Yes

The residues Ala 74, Ser 77, Glu 78, Val 96, Ile 175 and Val 171 interact with the ligands mostly by hydrophobic interactions with the ligands as shown in Table 4 and Figs. S41-S48.

As it has been observed that, the antimicrobials phloretin, naringenin, and quercetin bind strongly with those residues (Alguel et al., 2007).

2.6. ADMET

The ADMET parameters of the newly synthesized compounds (**3a-h**) were evaluated using the pkCSM (Pires et al., 2015) and AdmetLab (Ison et al., 2016) online tools. For a given compound a logBB < -1 considered poorly distributed to the brain. Positive result in AMES test suggests that compound could be mutagenic. Prediction of ADMET parameters are listed in Table 5.

Pharmacodynamics results indicated that compounds (**3a-h)** may prove good lead as antibacterial drugs by targeting DNA gyrase and transcriptional regulator (TtgR) enzyme. For drug formulation pharmacokinetic parameters are likewise a significant prospect and should be brought into thoughtfulness. The major properties studied for different synthesized compounds **(3a-h)** were to be acceptable and were incorporated in Table 5. The % oral intestinal drug absorption predicted for all compounds **3a-h** was highly satisfactory with a high percentage (> 90%), indicating their possibilities in oral drug formulation for the treatment of *staphyloccocu aureus* and *pseudomonas putida* infections. For the brain/blood partition coefficient of the compounds (**3a-h**) was predicted, thus, newly synthesized compounds presented little chance to cross the blood–brain barrier. In addition, rapid renal clearance is associated with small and hydrophilic compounds. The evaluation of the toxicity profile for compounds (**3a-h**) including the human ether-a-go-go related gene (hERG), AMES test, Max. Tolerated dose (human), Skin sensitization and Minnow toxicity indicate that acylhydrazones **3a-h** apparently do not have potential toxicity. Results of ADMET and bioavailability (Rule of Five) (Lipinski, 2004) as depicted in Tables 5 and 6, were within the acceptable limits for the designed compounds in both lipophilicity and solubility.

According to the *in vivo* pharmacodynamics results and *in silico* ADMET parameters, the newly synthetized compounds showed very interesting properties, in terms of intestinal adsorption, toxicity and Blood-brain barrier permeability; thus, it can be concluded that compounds **3a** and **3f** present good antibacterial activities against *staphyloccocu aureus* and *pseudomonas putida* infections, respectively. In addition, the present good drug-like characteristics and *in silico* ADMET parameters, consequently, they have more favorable properties as such and on further lead optimization may guide to novel compounds against *staphyloccocu aureus* and *pseudomonas putida* infections.

3. Conclusion

In this paper, novel N-acylhydrazone derivatives from acridone (**3a-k**) were synthesized by condensation of acridone acetohydrazide and various aldehyde. In the ^{1}H NMR and ^{13}C NMR spectra, two sets of signals were observed, which suggests that the compounds (**3a-k**) exists in two conformations (*E, trans* and *E, cis*). The antibacterial activity against *Escher-*

Table 6 Lipinski's properties of newly synthesized compounds.

Inhibitor	Property					
	Log*P*	H-bond acceptor	H-bond donor	Polar surface area (A^2)	Rotatable Bonds	Molecular weight (g/mol)
the assayed compounds						
3a	3.30	4	1	155.11	4	355.39
3d	3.95	4	1	165.41	4	389.84
3f	3.37	5	1	173.60	5	398.46
3g	3.21	6	1	169.76	5	400.39
3e	3.31	5	1	166.59	5	385.42
3b	3.01	5	2	159.90	4	371.39
3c	3.01	5	2	159.90	4	371.39
3h	3.01	6	2	171.38	5	401.42

ichia coli, *Klebsiella pneumoniae*, *Pseudomonas putida* and *Staphyloccocus aureus*, indicating that the introduction of acylhydrazone on the acridone ring increase the antibacterial activity. This results were supported by docking studies. The docking experiment tell us that compounds **3a** and **3f** are the most potent inhibitor of DNA gyrase of *Staphyloccocus aureus* and transcriptional regulator (TtgR) enzyme of *pseudomonas putida,* respectively.

4. Experimental

4.1. Materials

All materials were purchased from commercial suppliers. The ^{1}H, ^{13}C NMR spectra was recorded with Bruker Avance 300. Mass spectrometric measurements were recorded using Exactive™ Plus Orbitrap Mass Spectrometer.IR spectra were recorded using JASCO FT-IR 4100 spectrophotometer.

4.2. Antibacterial activity

The novel acylhydrazones (**3a-k**) were evaluated for their *in vitro* antibacterial activity by the disk diffusion method, the active compounds were subjected to the determination of the MIC, using the broth Microdilution method. The microorganisms utilized for the test were *Escherichia coli, Staphylococcus aureus, Pseudomonas putida* and *Klebsiella pneumonia*. They were collected from clinical isolates. Bacterial inoculums were prepared by subculturing microorganisms into MHB at 37 °C for 18 h and were diluted to approximately 10^6 CFU mL^{-1}. Initial solution with concentration 0.5 mg/mLof the compounds (**3a-k**) were prepared in DMF, further serial dilutions were made in the microplates and 100 µL of MHB containing each test microorganism were added to the microplate (Holetz et al., 2002; Olson et al., 2005; Sarkar et al., 2007), then incubated at 36 °C for 24 h. After incubation, 20 µL of TTC (0.04 mg/mL) were added to each microplate. The Color changes of TTC from colorless to red were accepted as microbial growth (Upadhya et al., 2013).

4.3. Molecular docking studies

Molecular docking of the compounds (**3a-h**) into the *S. aureus* DNA gyrase complex structure (PDB ID 3TTZ) (Sherer et al., 2011) and the transcriptional regulator (TtgR) enzyme of *p. putida* (PDB Code: 2UXI) (Alguel et al., 2007) was carried out using the SYBYL-X 2.0 molecular modeling package. The structures of 3TTZ and 2UXI in docking studies were downloaded from PDB. For protein preparation, the hydrogen atoms were added, water and impurities were removed. Different types of interactions between protein and the docked compounds (**3a-h**) were analyzed using Discovery Studio (Please, see the attached supplementary information**)**.

4.4. Synthesis

4.4.1. Ethyl 2-(9-oxoacridin-10(9H)-yl)acetate (*1*)

To a mixture of acridone (1 g, 5 mmol) and sodium hydride (90 mg, 7.2 mmol) in DMF (5 ml), ethyl 2-bromoacetate (1.2 g, 7.2 mmol) was added dropwise and the mixture was stirred at 60 °C for 3 h. After that, it was poured into crushed ice and the white yellow formed precipitate was recrystallized from ethanol-DMF.

Yellow solide, yield 75%, m.p. = 187 °C. IR (KBr) 3107, 2984, 2932, 1751, 1631, 1594, 1495 ^{1}H NMR (300 MHz, [D_6] DMSO, 25 °C, TMS): 8.36 (dd, J = 8.1, 1.5 Hz,2H, H1-H8), 7,95 (d, J = 8,7 Hz, 2H, H4, H5), 7.80 (td, J = 15.6, 6.9 1.5 Hz, 2H, H3, H6), 7.33 (t, J = 7.5 Hz, 2H, H2,H7), 5.75 (s, 2H, CH2), 4,33 (q, J = 7.2 Hz, 2H, CH2), 1,14 (t, J = 7.2 Hz, 3H,CH3). ^{13}C NMR (75 MHz, [D_6]DMSO, 25 °C, TMS):177.07, 168.64, 143.01, 142.23, 134.65, 127.13, 122.20, 122.00, 116.74, 61.89, 55.66, 15.12.

4.4.2. Synthesis of (9-oxo-9,10-dihydroacridin-10-yl) acetohydrazide (*2*)

To the compound **1** (1.12 g, 4 mmol), dissolved in DMSO (2 ml), was added hydrazine monohydrate (8 ml) and this mixture was refluxed for 24 hrs. Then the solvent was eliminated by evaporation and the obtained product was purified using recrystallization from DMF-ethanol.

Yellow solide yield: 76%; m.p > 300 °C; IR (KBr) 3320, 3084, 1670, 1640, 1570 cm^{-1}; ^{1}H NMR (300 MHz, [D_6] DMSO, 25 °C, TMS): 9.55 (s, 1H, NH), 8.34 (dd, J 8.1 Hz, 1.5 Hz, 2H), 7.80 (m, 2H), 7.62 (d, J = 8.1 Hz, 2H), 7.34 (td, 2H, J = 8.4, 1.5 Hz, 2H), 5.13 (s, 2H, CH_2), 4.35 (s, 2H, NH_2). ^{13}C NMR (300 MHz, DMSO d_6) δ (ppm): 177.23, 167.00, 142.98, 134.45, 126.98, 122.15, 121.89, 116.42 and 47.98.

*4.4.3. Synthesis of N-acylhydrazones derivatives from acridone (**3a-k**)*

An equimolar mixture of 2-(9-oxoacridin-10(9H)-yl)acetohydrazide **2** (0.1 g, 4 mmol) and aldehyde or ketone (4 mmol) was refluxed in ethanol for 2 hrs. The reaction mixture was filtered and the obtained solid was dried then recrystallized from a mixture of DMF and ethanol. Then purified by flash chromatography on silica gel using methanol/diethyl ether (1:3).

*4.4.4. N-benzylidene-2-(9-oxoacridin-10(9H)-yl) acetohydrazide (**3a**)*

Yellow solid; yield: 86%, mp > 300 °C. IR (KBr): 3226, 3070, 2984, 1680, 1640, 1605, 1495 cm^{-1}. ^1H NMR (300 MHz, [D_6]DMSO, 25 °C, TMS): 12.00 (s, 1H, NH, 27%), 11.95 (s, 1H, NH, 73%), 8.40 (dd, *J* = 8.0, 1.7 Hz, 2H), 8.32 (s, 1H, N═CH, 25%), 8.17 (s, 1H, N═CH, 75%), 7.84–7.65 (m, 6H), 7-52-7.45 (m, 3H), 7.39–7.34 (m, 2H), 5.79 (s, 2H, CH2, 73%), 5.34 (s, 2H, CH2, 27%). ^{13}C NMR (75 MHz, [D_6] DMSO, 25 °C, TMS): 177.22, 168.94, 164.34, 147.99, 144.87 142.98, 142.90, 134.63, 134.47, 130.59, 129.30, 127.61, 127.20, 122.09, 122.03, 121.90, 116.39, 48.50, 47.67. MS (ESI) for $C_{22}H_{17}N_3O_2$ $[M+1]^+$, calcd: 356,13, found: 356.13.

*4.4.5. N-(2-hydroxybenzylidene)-2-(9-oxoacridin-10(9H)-yl) acetohydrazide (**3b**)*

Yellow solid; yield: 74%, mp > 300 °C. IR (KBr): 3390, 3227, 3084, 2967, 1680, 1635, 1602, 1595, 1498 cm^{-1}. ^1H NMR (300 MHz, [D_6]DMSO, 25 °C, TMS):11.83 (s, 1H, NH, 40%), 11.78 (s, 1H, NH, 59%), 10.08 (s, 1H, OH), 8.38 (dd, *J* = 8.0, 1.7 Hz, 2H), 8.22 (s, 1H, CH═N, 41%), 8.07 (s, 1H, CH═N, 59%), 7.83 (ddd, *J* = 8.7, 6.9, 1.7 Hz, 2H), 7.71–7.66 (m, 4H), 7.40–7.34 (m, 2H), 6.88–6.83 (m, 2H), 5.71 (s, 2H, CH2, 59%), 5.28 (s, 2H, CH2, 41%). ^{13}C NMR (75 MHz, [D_6]DMSO, 25 °C, TMS): 177.22, 168.63, 164.01, 161.23, 147.23 144.54, 142.61, 142.53, 134.14, 128.86, 126.51, 124.99, 124.92, 121.53, 121.40, 114.89, 114.67, 48.51, 47.56. MS (ESI) for $C_{22}H_{17}N_3O_3$ $[M+1]^+$, calcd: 372,12, found: 372.13.

*4.4.6. N-(4-hydroxybenzylidene)-2-(9-oxoacridin-10(9H)-yl) acetohydrazide (**3c**)*

White solid; yield: 88%, mp > 300 °C. IR (KBr): 3368, 3226, 3081, 2980, 1685, 1631, 1610, 1596, 1497 cm^{-1}. ^1H NMR (300 MHz, [D_6]DMSO, 25 °C, TMS): 11.83 (s, 1H, NH, 24%), 11.77 (s, 1H, NH, 75%), 10.01 (s, 1H, OH), 8.40 (dd, *J* = 8.0, 1.7 Hz, 2H), 8.20 (s, 1H, CH═N, 26%), 8.07 (s, 1H, CH═N, 74%), 7.81 (ddd, *J* = 8.7, 6.9, 1.7 Hz, 2H), 7.74–7.52 (m, 4H), 7.44–7.34 (m, 2H), 6.86 (dd, *J* = 8.4, 5.8 Hz, 2H), 5.74 (s, 2H, CH2, 75%), 5.31 (s, 2H, CH2, 25%). ^{13}C NMR (75 MHz, [D_6]DMSO, 25 °C, TMS): 176.75, 168.01, 163.38, 159.38, 144.74, 142.51, 142.43, 134.14, 128.86, 126.51, 124.99, 124.92, 121.53, 121.40, 115.89, 115.67, 47.97, 47.14. MS (ESI) for $C_{22}H_{17}N_3O_3$ $[M+1]^+$, calcd: 372,12, found: 372.13.

*4.4.7. N-(4-chlorobenzylidene)-2-(9-oxoacridin-10(9H)-yl) acetohydrazide (**3d**)*

White solid; yield: 79%, mp > 300 °C. IR (KBr): 3207, 3079, 2970, 1680, 1633, 1604, 1599, 1493 cm^{-1}. ^1H NMR (300 MHz, [D_6]DMSO, 25 °C, TMS): 12.10 (s,1H, NH, 26%)12.03 (s,1H, NH, 74%), 8.40 (dd, *J* = 8.1, 1.7 Hz, 2H), 8.31 (s, 1H, N═CH, 26%), 8.15 (s, 1H, N═CH, 74%), 7.90–7.83 (m, 2H), 7.79–7.76 (m, 2H), 7.71–7.64 (m, 2H), 7.56–7.52 (m, 2H), 7.40–7.33 (m, 2H), 5.79 (s, 2H, CH2, 74%), 5.17 (s, 2H, CH2, 26%). ^{13}C NMR (75 MHz, [D_6]DMSO, 25 °C, TMS):176.74, 168.51, 166.51, 146.24, 143.08, 142.48, 134.51, 134.13, 133.95, 132.95, 128.86, 128.77, 126.49, 121.66, 121.56, 121.40, 115.91, 47.49, 47.22. MS (ESI) for $C_{22}H_{16}ClN_3O_2$ $[M+1]^+$, calcd: 390,09, found: 390.09.

*4.4.8. N-(4-methoxybenzylidene)-2-(9-oxoacridin-10(9H)-yl) acetohydrazide (**3e**)*

Yellow solid; yield: 90%, mp > 300 °C. IR (KBr): 3210, 3281, 2952, 1680, 1637, 1603, 1493 cm^{-1}. ^1H NMR (300 MHz, [D_6] DMSO, 25 °C, TMS): 11.82 (s, 1H, NH, 26%), 11.78 (s, 1H, NH, 74%), 8.36 (dd, *J* = 8.0, 1.7 Hz, 2H), 8.22 (s, 1H, N═CH, 25%), 8.07 (s, 1H, N═CH, 75%), 7.82–7.59 (m, 6H), 7.33 (m, 2H), 7.01 (dd, *J* = 8.7, 2H), 5.71 (s, 2H, CH2, 75%), 5.28 (s, 2H, CH2, 25%), 3.79(s, 3H, OCH3). ^{13}C NMR (75 MHz, [D_6]DMSO, 25 °C, TMS): 177.20, 168.62, 164.00, 161.30, 147.91, 144.79, 142.93, 134.59, 129.19, 127.00, 122.11, 122.05, 121.86, 116.38, 114.77, 55.79, 48.51, 47.65. MS (ESI) for $C_{23}H_{19}N_3O_3$ $[M+1]^+$, calcd: 386,14, found: 386.14.

*4.4.9. N-(4-(dimethylamino)benzylidene)-2-(9-oxoacridin-10 (9H)-yl)acetohydrazide (**3f**)*

White solid; yield: 74%, mp > 300 °C. IR (KBr): 3196, 3097, 2980, 1681, 1639, 1605, 1490 cm^{-1}. ^1H NMR (300 MHz, [D_6] DMSO, 25 °C, TMS): 11.71 (s, 1H, NH, 27%), 11.68 (s, 1H, NH, 73%), 8.38 (dd, *J* = 8.0, 1.7 Hz, 2H), 8.15 (s, 1H, N═CH, 27%), 8.03 (s, 1H, N═CH, 73%), 7.82 (tdd, *J* = 8.7, 6.9, 1.8 Hz, 2H), 7.75–7.53 (m, 4H), 7.44–7.30 (m, 2H), 6.76 (dd, *J* = 9.1, 2.7 Hz, 2H), 5.72 (s, 2H, CH2, 74%), 5.30 (s, 2H, CH2, 26%), 2.98 (s, 6H, NCH3). ^{13}C NMR (75 MHz, [D_6]DMSO, 25 °C, TMS):176.73, 167.73, 151.47, 145.30, 142.53, 142.45, 134.12, 128.48, 128.39, 126.51, 121.61, 121.37, 121.25, 115.90, 111.72, 47.11. MS (ESI) for $C_{24}H_{22}N_4O_2$ $[M+1]^+$, calcd: 399,17, found: 399.17.

*4.4.10. N-(4-nitrobenzylidene)-2-(9-oxoacridin-10(9H)-yl) acetohydrazide (**3g**)*

Yellow solid; yield: 86%, mp > 300 °C. IR (KBr): 3234, 3090, 2962, 1693, 1635, 1611, 1593, 1521, 1493 cm^{-1}. ^1H NMR (300 MHz, [D_6]DMSO, 25 °C, TMS): 12.31 (s, 1H, NH, 26%), 12.24 (s, 1H, NH, 74%), 8.43 (s, 1H, N═CH, 25%), 8.41 (dd, *J* = 8.0, 1.7 Hz, 2H), 8.33(m,2H), 8.27 (s, 1H, N═CH, 75%), 8.14–8.00 (m, 2H), 7.87–7.67 (m, 4H), 7.41–7.35 (m, 2H), 5.85 (s, 2H, CH2, 74%), 5.39 (s, 2H, CH2, 25%). ^{13}C NMR (75 MHz, [D_6]DMSO, 25 °C, TMS): 178.41, 168.89, 163.73, 147.87, 145.16, 142.42, 140.30, 134.16, 131.00, 128.10, 126.55, 126.41, 124.95, 123.94, 121.58, 121.46, 120.98, 115.90, 48.32, 47.29. MS (ESI) for $C_{22}H_{16}N_4O_4$ $[M+1]^+$, calcd: 401,11, found: 401,12.

*4.4.11. N-(4-hydroxy-3-methoxybenzylidene)-2-(9-oxoacridin-10(9H)-yl)acetohydrazide (**3h**)*

Yellow solid; yield: 77%, mp > 300 °C. IR (KBr): 3327, 3221, 3092, 2986, 2630, 1677, 1635, 1604, 1495 cm^{-1}. ^1H NMR (300 MHz, [D_6]DMSO, 25 °C, TMS): 11.82 (s, 1H, NH,

27%), 11.78 (s, 1H, NH, 73%), 9.58 (s, 1H, OH), 8.41 (dd, J = 8.0, 1.7 Hz, 2H), 8.20 (s, 1H, N=CH, 25%), 8.06 (s, 1H, N=CH, 75%), 7.85–7.79 (m, 2H), 7.68–7.63 (m, 2H), 7.46–7.11 (m, 4H), 7.89 (m, *1*H), 5.77 (s, 2H, CH2, 73%), 5.32 (s, 2H, CH2, 27%), 3.83(s, 3H, OCH3). ^{13}C NMR (75 MHz, [D_6]DMSO, 25 °C, TMS):176.73, 168.06, 163.40, 148.95, 148.01, 145.61, 144.82, 142.54, 142.46, 134.11, 126.51, 125.45, 121.72, 121.56, 121.38, 115.93, 115.49, 115.49, 109.68, 55.67, 47.28. MS (ESI) for $C_{23}H_{19}N_3O_4$ $[M+1]^+$, calcd: 402,13, found: 402.12.

*4.4.12. 2-(9-oxoacridin-10(9H)-yl)-N'-(propan-2-ylidene) acetohydrazide (**3k**)*

Yellow solid; yield: 68%, mp > 300 °C. IR (KBr): 3208, 3036, 2934, 1668, 1632, 1598, 1493 cm^{-1}. ^{1}H NMR (300 MHz, [D_6] DMSO, 25 °C, TMS): 10.77 (s, 1H, NH, 27%), 10.66 (s, 1H, NH, 73%), 8.38 (dd, J = 8.0, 1.7 Hz, 2H), 7.89–7.75 (m, 2H), 7.67 (d, J = 8.8 Hz, 1H), 7.57 (d, J = 8.7 Hz, 1H), 7.36 (t, J = 7.4 Hz, 2H), 5.59 (s, 2H, CH2, 73%), 5.36 (s, 2H, CH2, 27%), 2.06 (s, 3H, CH3), 1.99 (s, 3H, CH3). ^{13}C NMR (75 MHz, [D_6]DMSO, 25 °C, TMS): 176.71, 168.31, 163.38, 152.33, 142.42, 134.09, 126.50, 121.54, 121.34, 115.89, 115.75, 47.56, 47.29, 25.29, 17.29.

Declaration of Competing Interest

The authors declare that they have no known competing financial interests or personal relationships that could have appeared to influence the work reported in this paper.

Appendix A. Supplementary material

Supplementary data to this article can be found online at https://doi.org/10.1016/j.arabjc.2020.05.034.

References

Aarjane, M., Slassi, S., Amine, A., 2020. Novel highly selective and sensitive fluorescent sensor for copper detection based on N-acylhydrazone acridone derivative. J. Mol. Struct. 1199, 126990. https://doi.org/10.1016/j.molstruc.2019.126990.

Aarjane, M., Slassi, S., Tazi, B., Maouloua, M., Amine, A., 2019. Novel series of acridone-1,2,3-triazole derivatives: microwave-assisted synthesis, DFT study and antibacterial activities. J. Chem. Sci. 131, 85. https://doi.org/10.1007/s12039-019-1653-2.

Abubakar, U., Muhammad, H.T., Sulaiman, S.A.S., Ramatillah, D. L., Amir, O., 2020. Knowledge and self-confidence of antibiotic resistance, appropriate antibiotic therapy, and antibiotic stewardship among pharmacy undergraduate students in three Asian countries. Pharm. Teach. Learn Curr. https://doi.org/10.1016/j.cptl.2019.12.002.

Alguel, Y., Meng, C., Terán, W., Krell, T., Ramos, J.L., Gallegos, M.-T., Zhang, X., 2007. Crystal structures of multidrug binding Protein TtgR in complex with antibiotics and plant antimicrobials. J. Mol. Biol. 369, 829–840. https://doi.org/10.1016/j.jmb.2007.03.062.

Alves, M., Froufe, H., Costa, A., Santos, A., Oliveira, L., Osório, S., Abreu, R., Pintado, M., Ferreira, I., 2014. Docking studies in target proteins involved in antibacterial action mechanisms: extending the knowledge on standard antibiotics to antimicrobial mushroom compounds. Molecules 19, 1672–1684. https://doi.org/10.3390/molecules19021672.

Antibiotic Development: the Battle to Overcome Antibiotic Resistance, 1984. InPharma 437, 4–4. https://doi.org/10.1007/bf03315506.

Areas, E.S., da Bronsato, B.J.S., Pereira, T.M., Guedes, G.P., da Miranda, F.S., Kümmerle, A.E., da Cruz, A.G.B., Neves, A.P., 2017. Novel CoIII complexes containing fluorescent coumarin-N-acylhydrazone hybrid ligands: Synthesis, crystal structures, solution studies and DFT calculations. Spectrochim. Acta - Part A Mol. Biomol. Spectrosc. 187, 130–142. https://doi.org/10.1016/j.saa.2017.06.031.

Baig, N., Singh, R.P., Chander, S., Jha, P.N., Murugesan, S., Sah, A. K., 2015. Synthesis, evaluation and molecular docking studies of amino acid derived N-glycoconjugates as antibacterial agents. Bioorg. Chem. 63, 110–115. https://doi.org/10.1016/j.bioorg.2015.10.002.

Cerqueira, J.V., Meira, C.S., de Santos, E.S., de Aragão França, L.S., Vasconcelos, J.F., Nonaka, C.K.V., de Melo, T.L., dos Santos Filho, J.M., Moreira, D.R.M., Soares, M.B.P., 2019. Anti-inflammatory activity of SintMed65, an N-acylhydrazone derivative, in a mouse model of allergic airway inflammation. Int. Immunopharmacol. 75, 105735. https://doi.org/10.1016/j.intimp.2019.105735.

Coimbra, E.S., Nora de Souza, M.V., Terror, M.S., Pinheiro, A.C., da Trindade Granato, J., 2019. Synthesis, biological activity, and mechanism of action of new 2-pyrimidinyl hydrazone and N-acylhydrazone derivatives, a potent and new classes of antileishmanial agents. Eur. J. Med. Chem. 184, 111742. https://doi.org/10.1016/j.ejmech.2019.111742.

Dehestani, L., Ahangar, N., Hashemi, S.M., Irannejad, H., Honarchian Masihi, P., Shakiba, A., Emami, S., 2018. Design, synthesis, in vivo and in silico evaluation of phenacyl triazole hydrazones as new anticonvulsant agents. Bioorg. Chem. 78, 119–129. https://doi.org/10.1016/j.bioorg.2018.03.001.

dos Santos Filho, J.M., de Queiroz e Silva, D.M.A., Macedo, T.S., Teixeira, H.M.P., Moreira, D.R.M., Challal, S., Wolfender, J.L., Queiroz, E.F., Soares, M.B.P., 2016. Conjugation of N-acylhydrazone and 1,2,4-oxadiazole leads to the identification of active antimalarial agents. Bioorganic Med. Chem. 24, 5693–5701. https://doi.org/10.1016/j.bmc.2016.09.013.

Gensicka-Kowalewska, M., Cholewiński, G., Dzierzbicka, K., 2017. Recent developments in the synthesis and biological activity of acridine/acridone analogues. RSC Adv. https://doi.org/10.1039/c7ra01026e.

Hamzi, I., Barhoumi-Slimi, T.M., Abidi, R., 2016. Synthesis, characterization, and conformational study of acylhydrazones of α, β-unsaturated aldehydes. Heteroat. Chem. 27, 139–148. https://doi.org/10.1002/hc.21310.

He, Haifeng, Xia, H., Xia, Q., Ren, Y., He, Hongwu, 2017. Design and optimization of N-acylhydrazone pyrimidine derivatives as E. coli PDHc E1 inhibitors: Structure-activity relationship analysis, biological evaluation and molecular docking study. Bioorganic Med. Chem. 25, 5652–5661. https://doi.org/10.1016/j.bmc.2017.08.038.

Himmelreich, U., Tschwatschal, F., Borsdorf, R., 1993. NMR-spektroskopische Untersuchungen an Derivaten des 2,4-Dichlorphenoxyessigsäurehydrazids. Monatshefte für Chemie Chem. Mon. 124, 1041–1051. https://doi.org/10.1007/BF00814150.

Holetz, F.B., Pessini, G.L., Sanches, N.R., Cortez, D.A.G., Nakamura, C.V., Filho, B.P.D., 2002. Screening of some plants used in the Brazilian folk medicine for the treatment of infectious diseases. Mem. Inst. Oswaldo Cruz 97, 1027–1031. https://doi.org/10.1590/s0074-02762002000700017.

Inam, A., Siddiqui, S.M., Macedo, T.S., Moreira, D.R.M., Leite, A.C. L., Soares, M.B.P., Azam, A., 2014. Design, synthesis and biological evaluation of 3-[4-(7-chloro-quinolin-4- yl)-piperazin-1-yl]-propionic acid hydrazones as antiprotozoal agents. Eur. J. Med. Chem. 75, 67–76. https://doi.org/10.1016/j.ejmech.2014.01.023.

Ison, J., Rapacki, K., Ménager, H., Kalaš, M., Rydza, E., Chmura, P., Anthon, C., Beard, N., Berka, K., Bolser, D., Booth, T., Bretaudeau, A., Brezovsky, J., Casadio, R., Cesareni, G., Coppens,

F., Cornell, M., Cuccuru, G., Davidsen, K., Vedova, G. Della, Dogan, T., Doppelt-Azeroual, O., Emery, L., Gasteiger, E., Gatter, T., Goldberg, T., Grosjean, M., Grüning, B., Helmer-Citterich, M., Ienasescu, H., Ioannidis, V., Jespersen, M.C., Jimenez, R., Juty, N., Juvan, P., Koch, M., Laibe, C., Li, J.-W., Licata, L., Mareuil, F., Mičetić, I., Friborg, R.M., Moretti, S., Morris, C., Möller, S., Nenadic, A., Peterson, H., Profiti, G., Rice, P., Romano, P., Roncaglia, P., Saidi, R., Schafferhans, A., Schwämmle, V., Smith, C., Sperotto, M.M., Stockinger, H., Vařeková, R.S., Tosatto, S.C. E., de la Torre, V., Uva, P., Via, A., Yachdav, G., Zambelli, F., Vriend, G., Rost, B., Parkinson, H., Løngreen, P., Brunak, S., 2020. Tools and data services registry: a community effort to document bioinformatics resources. Nucleic Acids Res. 44, D38–D47. https://doi.org/10.1093/nar/gkv1116.

Kheradmand, A., Navidpour, L., Shafaroodi, H., Saeedi-Motahar, G., Shafiee, A., 2013. Design and synthesis of niflumic acid-based N-acylhydrazone derivatives as novel anti-inflammatory and analgesic agents. Med. Chem. Res. 22, 2411–2420. https://doi.org/10.1007/s00044-012-0235-3.

Kudryavtseva, T.N., Sysoev, P.I., Popkov, S.V., Nazarov, G.V., Klimova, L.G., 2015. Synthesis and antimicrobial activity of some acridone derivatives bearing 1,3,4-thiadiazole and 1,2,4-triazole moieties. Russ. Chem. Bull. 64, 445–450. https://doi.org/10.1007/s11172-015-0884-8.

Kumar, A., Srivastava, K., Raja Kumar, S., Puri, S.K., Chauhan, P. M.S., 2009. Synthesis of 9-anilinoacridine triazines as new class of hybrid antimalarial agents. Bioorganic Med. Chem. Lett. 19, 6996–6999. https://doi.org/10.1016/j.bmcl.2009.10.010.

Liao, Z., Liu, Y., Han, S.F., Wang, D., Zheng, J.Q., Zheng, X.J., Jin, L.P., 2017. A novel acylhydrazone-based derivative as dual-mode chemosensor for Al3+, Zn2+ and Fe3+ and its applications in cell imaging. Sensors Actuators, B Chem. 244, 914–921. https://doi.org/10.1016/j.snb.2017.01.074.

Lipinski, C.A., 2004. Lead- and drug-like compounds: the rule-of-five revolution. Drug Discov. Today Technol. 1, 337–341. https://doi.org/10.1016/j.ddtec.2004.11.007.

Olson, C.R., Balasubramaniam, T., Shrum, J., Nord, T., Taylor, P.L., Burrell, R.E., 2005. Novel antimicrobial activity of nanocrystalline silver dressings, in: Proceedings - 2005 International Conference on MEMS, NANO and Smart Systems, ICMENS 2005. pp. 129–131. https://doi.org/10.1109/ICMENS.2005.90.

Pires, D.E.V., Blundell, T.L., Ascher, D.B., 2015. pkCSM: Predicting small-molecule pharmacokinetic and toxicity properties using graph-based signatures. J. Med. Chem. 58, 4066–4072. https://doi.org/10.1021/acs.jmedchem.5b00104.

Podyachev, S.N., Litvinov, I.A., Shagidullin, R.R., Buzykin, B.I., Bauer, I., Osyanina, D.V., Avvakumova, L.V., Sudakova, S.N., Habicher, W.D., Konovalov, A.I., 2007. Structure and spectroscopic characteristics of 4-tert-butylphenoxyacetylhydrazones of arylaldehydes. Spectrochim. Acta - Part A Mol. Biomol. Spectrosc. 66, 250–261. https://doi.org/10.1016/j.saa.2006.02.049.

Sarigöl, D., Yüksel, D., Okay, G., Uzgören-Baran, A., 2015. Synthesis and structural studies of acyl hydrazone derivatives having tetrahydrocarbazole moiety. J. Mol. Struct. 1086, 146–152. https://doi.org/10.1016/j.molstruc.2014.12.092.

Sarkar, S., Jana, A.D., Samanta, S.K., Mostafa, G., 2007. Facile synthesis of silver nano particles with highly efficient anti-microbial property. Polyhedron 26, 4419–4426. https://doi.org/10.1016/j.poly.2007.05.056.

Sepúlveda, C.S., García, C.C., Fascio, M.L., D'Accorso, N.B., Docampo Palacios, M.L., Pellón, R.F., Damonte, E.B., 2012. Inhibition of Junin virus RNA synthesis by an antiviral acridone derivative. Antiviral Res. 93, 16–22. https://doi.org/10.1016/j.antiviral.2011.10.007.

Sherer, B.A., Hull, K., Green, O., Basarab, G., Hauck, S., Hill, P., Loch, J.T., Mullen, G., Bist, S., Bryant, J., Boriack-Sjodin, A., Read, J., DeGrace, N., Uria-Nickelsen, M., Illingworth, R.N., Eakin, A.E., 2011. Pyrrolamide DNA gyrase inhibitors: Optimization of antibacterial activity and efficacy. Bioorg. Med. Chem. Lett. 21, 7416–7420. https://doi.org/10.1016/j.bmcl.2011.10.010.

Tillequin, F., Koch, M., 2005. De l'acronycine aux dérivés de la benzo[b]acronycine: Conception et développement d'une nouvelle série d'antitumoraux. Ann. Pharm. Fr. 63, 35–43. https://doi.org/10.1016/s0003-4509(05)82249-7.

Tripos International, 2012. Sybyl molecular modeling software.

Tsafack, A., Loyevsky, M., Ponka, P., Cabantchik, Z.I., 1996. Mode of action of iron (III) chelators as antimalarials. IV. Potentiation of desferal action by benzoyl and isonicotinoyl hydrazone derivatives. J. Lab. Clin. Med. 127, 574–582. https://doi.org/10.1016/S0022-2143(96)90148-1.

Upadhya, V., Hegde, H.V., Bhat, S., Kholkute, S.D.S.A.G., Potsangbam, L., Ningombam, S., Laitonjam, W.S., Navarro, V., Villarreal, M.L., Rojas, G., Lozoya, X., Kakar, D.N., 2013. Microsoft Word - TK- 1563_JAN_.doc - IJTK 9(1), 9–17.pdf. J. Ethnobiol. Ethnomed. 7, 61–63. https://doi.org/10.1186/1746-4269-10-49.

Wang, X.L., Zhang, Y. Bin, Tang, J.F., Yang, Y.S., Chen, R.Q., Zhang, F., Zhu, H.L., 2012. Design, synthesis and antibacterial activities of vanillic acylhydrazone derivatives as potential β-ketoacyl-acyl carrier protein synthase III (FabH) inhibitors. Eur. J. Med. Chem. 57, 373–382. https://doi.org/10.1016/j.ejmech.2012.09.009.

Zarei-Baygi, A., Harb, M., Wang, P., Stadler, L.B., Smith, A.L., 2020. Microbial community and antibiotic resistance profiles of biomass and effluent are distinctly affected by antibiotic addition to an anaerobic membrane bioreactor. Sci. Water Res. Technol. Environ. https://doi.org/10.1039/c9ew00913b.